Refractoriness in Poisson and Gaussian First-order Neural Nets with Chemical Markers

ELENI FOURNOU[1], PANOS ARGYRAKIS[2],[*] and PHOTIOS A. ANNINOS[3]
[1]*Department of Applied Sciences, Technological Education Institution (TEI) of Thessaloniki, 57400 Sindos, Greece. e-mail: efournou@gen.teithe.gr*
[2]*Department of Physics, University of Thessaloniki, 54124 Thessaloniki, Greece. e-mail: panos@physics.auth.gr*
[3]*Department of Medical Physics, University of Thraki, 68100 Alexandroupolis, Greece. e-mail: anninos@axd.forthnet.gr*

Abstract. In this work first order probabilistic Poisson and Gaussian neural nets with chemical markers are investigated, analytically and by computer simulations. The investigation of steady-state behavior of these systems is extended here to systems in which the refractory period is assigned to be 1 for all or some of the subpopulations of the net, whereas the remainder are characterized by zero refractory periods. The interest is focused on the effects of refractoriness on the neural activities. Results obtained show the existence of several critical points at high initial activities, which are a consequence of the nonzero refractory periods. For these points a larger initial activity, above a certain critical level, results in the reduction of activity to a lower stable steady-state, instead of the highest one. We also find that in the Gaussian nets each critical point is lower than the corresponding one as in the Poisson nets. Finally, a discussion of the results is made.

Key words. chemical markers, neural nets, refractoriness

1. Introduction

An area of considerable importance is that of biological nets, i.e. models of nets that try to imitate the human or other living brain structure and functions in an effort to understand such vital processes as memory, learning, understanding, etc. Widely used models (not an exhaustive list) include the early pioneer work of McCulloch and Pitts of assemblies of neurons as logical decision elements [1], the mathematical formalism of Caianiello of the 'neuronic equation' [2], and the probabilistic neural structure [3–6] that monitor the neural activity, i.e. the fraction of neurons that become active per unit time. These models have been quite successful towards our understanding of the above mentioned functions. In these models a network is made of a large number of neurons (the elementary unit), which are interconnected according to some rules. As each unit has several connections, and there is a large number of units, it is quickly realized that the number of connections grows very fast, making the task of calculations quite difficult. But it should

---

[*]Corresponding author.

be realised that it is exactly this complicated connectivity structure that produces the collective properties that neural nets possess.

The probabilistic neural nets initially were quite simple [5,6], but later got more involved [7–12], and incorporate today several advanced characteristics met in actual neural networks. Their theoretical basis is the binomial distribution, as one tries to attribute some specific properties to a fraction of units out of the total population. The mathematical formalism is quite involved, but straightforward. Alternatively, we use a Monte Carlo simulation model to verify the analytical findings. The two methods are used interchangeably, and direct comparison yields satisfactory agreement.

In previous studies [9] we investigated the dynamical behavior of isolated neural nets with chemical markers and high interneuronal connectivities and the relationship between structure, as expressed in patterns of interneuronal synaptic connectivity, and 'spontaneous' activity. The Poisson and Gaussian distributions of the connectivities of the constituent neurons were used. This investigation was extended then to non-isolated netlets with markers, where it was assumed that the netlet under consideration is attached to a cable of afferent fibers receiving through it sustained inputs from another netlet with the same structure. Later [11], a generalization was attempted by including the possibility that different subsystems of a neural net have different connectivity patterns, given by the appropriate distribution laws, Poisson or Gaussian, assigned to sections with different markers. Thus, the overall net acquired a hybrid character.

In the present study, the dynamical behavior of isolated neural nets with chemical markers is further investigated. Here, our interest is focused on the effect of refractoriness on the dynamical steady-state behavior of pure Poisson or Gaussian netlets. We consider nets in which r, the refractory period, is assigned a value of $r = 1$ to all or some of their subsystems, whereas the remainder are characterized by zero refractory period. It is shown here that the nonzero refractory period of the constituent subsystems gives some interesting specific features on the dynamical behavior of the neural structures. These features are related with the subsequent total activity of the net for high level initial activities. Due to the nonzero refractory period, one or more critical points emerge at high levels for the initial activities, which control the subsequent neural activity. Furthermore, if all subsystems of the net have refractory periods $r = 1$, then all the stable steady-states for the total neural activity are held in levels lower than the value of $a_{ss} = 0.5$.

2.   Material and Methods

2.1.   ASSUMPTIONS AND DEFINITIONS

The present investigation makes use of the neural net models developed in our previous work [7,9]. It was assumed that neural nets are constructed of discrete sets of randomly interconnected neurons with similar structure and function, which are

termed 'netlets' [6], but the neural connections are set up by means of chemical markers carried by the individual cells, according to the theory of neural specificity [13–15]. Thus, the neural population of the netlet is treated as a set of subpopulations of neurons, each of then characterized by a specific chemical marker. The neurons are bistable elements, as was postulated by McCullogh and Pits [1], and operate synchronously at discrete times.

It is assumed that if a neuron fires at time t, it produces the appropriate PSPs (Post-Synaptic Potentials) after a fixed time interval called the synaptic delay, τ. All PSPs arriving at a neuron are summed instantly and, if they exceed the specified threshold, will cause the neuron to fire. After firing neurons are insensitive to further stimulation for a period of time called the 'refractory period'. Thus, the neurons are characterized by the absolute refractory property, r, the firing threshold, θ, and the synaptic delay, τ. It is assumed here that the refractory period is greater than the synaptic delay, but less than twice the synaptic delay. The parameter r may take in general any integer value. For our purposes r was given the value $r = 1$ when refractoriness is assumed, and $r = 0$ otherwise. From these assumptions it follows that if a number of neurons fire simultaneously at time t, then all neural activity resulting from this initial activity will be restricted to times $t + \tau, t + 2\tau, \ldots,$ etc. The assumed time constraints (synaptic delay, refractory period, and summation time) are such that the neural activity depends exclusively on the activity at the preceding firing interval. Thus, the dynamics of the netlet is a Markov process and the mathematical expression for the activity is given by a first order finite difference equation. The neural nets that follow such equation are termed first order nets.

2.2. LIST OF SYMBOLS

The subscript j is a marker label and indicates the properties of a subpopulation in the network characterized by the jth marker.

Structural parameters of the neural net

τ synaptic delay
A total number of neurons in the network
N number of markers (subsystems)
m_j fraction of neurons carrying the jth marker in the network
h_j fraction of inhibitory neurons
μ_j^+ the average number of neurons receiving excitatory post-synaptic potentials (EPSPs) from one excitatory neuron
μ_j^- the average number of neurons receiving inhibitory post-synaptic potentials (IPSPs) from one inhibitory neuron
K_j^+ the size of PSP produced by an excitatory neuron
K_j^- the size of PSP produced by an inhibitory neuron
ϑ_j firing threshold of neurons of the jth marker

Dynamical parameters

n an integer giving the number of elapsed synaptic delays

a_n the activity, i.e. the fractional number of active neurons in the netlet
        at time $t = n\tau$

2.3. MATHEMATICAL FORMALISM

A neural net with N markers is assumed to be constructed of A formal neurons. A fraction $h(0 < h < 1)$ of them are inhibitory neurons while the rest are excitatory. Each neuron receives, on the average, μ^+ EPSPs and μ^- IPSPs. The size of the PSP produced by an excitatory (inhibitory) unit is $K^+(K^-)$.

The dynamic variable of interest is the neural activity a_n, which is the fraction of neurons in the netlet (out of the total) that are active at time $t = n\tau$. This quantity is a scalar and does not specify which particular neurons are firing in the netlet. The quantity a_n at time $t = n\tau$ depends exclusively on the firing record of the netlet at time $t = (n-1)\tau$, i.e., the previous time unit. Assuming that a_n is the netlet activity at time $t = n\tau$, then the expectation value of activity $\langle a_{n+1} \rangle$ for a netlet of A neurons and N markers at time $t = (n+1)\tau$ is given by equation

$$\langle a_{n+1} \rangle = (1 - a_n) \sum_{j=1}^{N} m_j P_j \tag{1}$$

where $m_j (j = 1, 2, \ldots, N)$ is the fraction of neurons out of the total, carrying the jth marker in the netlet and $m_1 + m_2 + \cdots + m_N = 1$. The quantity P_j, which is the probability that a neuron of the jth marker receives a total PSP which exceeds its threshold θ_j, may be expressed in terms of a Poisson or Gaussian distribution law of the number of excitatory and inhibitory inputs to a cell. The expectation value of activity $\langle a_{n+1} \rangle$ will also depend on whether there is refractoriness or not ($r = 1$ or $r = 0$). Thus, the factor $(1 - a_n)$ in this equation is neglected if no refractoriness ($r = 0$) is assumed.

For the Poisson approximation [7,9], P_j is given by the equation:

$$P_j = P_{Pj} = \sum_{I=0}^{I_{\max,j}} \left(1 - \sum_{L=0}^{\eta'_j - 1} P_{L,j} \right) Q_{I,j} \tag{2}$$

where $P_{L,j}$, and $Q_{I,j}$ are the probabilities that a neuron of the jth marker will receive L-EPSPs and I-IPSPs, respectively, at time $t = (n+1)\tau$. The upper limits $I_{\max,j}$ and η'_j are the total numbers of the inhibitory inputs and the minimum number of excitatory inputs necessary to trigger a neuron, respectively. Equation (2) results by adding all probabilities for all combinations of thresholds and PSPs that produce firing.

If the average number of active inputs per neuron becomes sufficiently large, the number of PSPs per neuron will follow a Gaussian distribution. In this case, P_j is

given by the equation [9]:

$$P_j = P_{Gj} = \frac{1}{\sqrt{2\pi}} \int\limits_{x_{j,n+1}}^{\infty} e^{\frac{-x^2}{2}} \, dx \tag{3}$$

where

$$x_{j,n+1} = \frac{\theta_j - \bar{e}_{j,n+1}}{\delta_{j,n+1}} \tag{4}$$

$$\bar{e}_{j,n+1} = a_n m_j \left[\mu_j^+ (1 - h_j) K^+ + \mu_j^- h_j K^- \right] \tag{5}$$

and

$$\delta_{j,n+1}^2 = a_n m_j \left[\mu_j^+ (1 - h_j)(K^+)^2 + \mu_j^- h_j (K^-)^2 \right] \tag{6}$$

2.4. COMPUTER SIMULATION MODEL

We use Monte Carlo calculations for the net structure and properties, by assigning specific values to the parameters of Section 2.2 (see below). We can produce pictorials of the microstates of the system at any time, with useful insight at the intermediate excitation structures. Given the structural parameters of a network of A neurons and N markers, the appropriate neuronal connectivity matrix $\{k_{ij}\}$ is first constructed. Each element k_{ij} denotes the synaptic strength of the connection from j to i neuron (coupling coefficient). This may take either positive or negative values depending on the type of the synaptic neuron (excitatory or inhibitory, respectively). The threshold (θ) as well some other macroscopic parameters ($K^\pm, \mu^\pm$) are considered to vary randomly between a maximum and a minimum value in order to produce more realistic behavior. After establishing all desired interconnections, the network is activated by specifying the set of neurons which are randomly taken to be active at time $t = 0$. One synaptic delay later, all neurons linked to them will receive the appropriate inputs. The inputs arriving at a neuron are summed instantly and if the sum exceeds the neuron threshold, then the neuron will fire. All active neurons at the next time step are specified. The firing neurons for the time step $t = n\tau$ define the state vector $\mathbf{a_n}$. Refractoriness of neurons is taken into account by imposing that a neuron firing at time $t = n\tau$ cannot fire at the next time $t = (n+1)\tau$.

3. Results and Discussion

The results shown below are taken on the basis of Equation (1) with the appropriate expressions of P_j according to Poisson (Eq. (2)) or Gaussian (Eq. (3)) approximation. For the sake of clarity, in the examples presented here we consider isolated

neural nets with two and three markers and appropriate combination of other parameters, in an effort to exhibit the effect of refractory period on the dynamical behavior of the net. We used

1. Plots of the expectation value of activity as a function of the preceding activity, i.e. $\langle a_{n+1} \rangle$ versus a_n
2. Time course plots of neural activity, and
3. Time delay plots, i.e. plots which give the time that it takes for a netlet to reach a stable steady-state (t_{ss}) as a function of the initial activity.

We examined the case of a netlet of A neutrons with two markers, $m_\alpha = 0.25$, $m_b = 0.75$ and refractory periods $r_\alpha = 0$ and $r_b = 1$. Plots of $\langle a_{n+1} \rangle$ versus a_n for both approximations Poisson and Gaussian are shown in Figure 1. The contribution to the total activity of each marker and simulation results are also depicted here. For the chosen set of parameters we obtain a two-modal curve [8] of the total activity for both approximations, Poisson and Gaussian. This curve labeled T (total activity) in the range $a_n = 0$–0.6 has two modes (waves) along the corresponding line. We can see here three stable steady-states, the zero level state $a_{P\text{ss}}^{\text{o}} = a_{G\text{ss}}^{\text{o}} = 0$, and two nonzero states, which are the crossing points of the curve with the straight line at $45°$ slope coming from above. We also have two unstable states, equivalently, at the crossing points of the curve with the straight line at $45°$ slope coming from below.
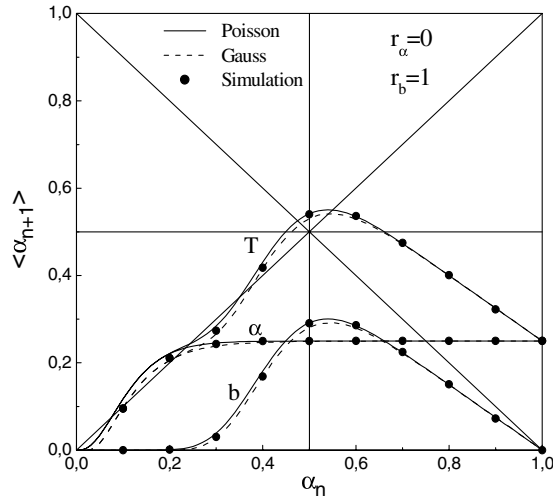

Figure 1. Expectation value of the total neural activity $\langle a_{n+1} \rangle$ vs preceding activity a_n for an isolated netlet with two chemical markers, a and b, with $m_\alpha = 0.25$; $m_b = 0.75$; $\mu_\alpha^+ = 102$, $\mu_b^+ = 62$; $h = 0$; $\vartheta_\alpha = 3$, $\vartheta_b = 20$; $r_a = 0$, $r_b = 1$; $K^+ = 1$. The curves a and b represent the activities of each marker, whereas T gives the total activity of the netlet. The solid lines are used for the Poisson approximation whereas the dashed lines for the Gaussian one. The solid dots are simulation results.
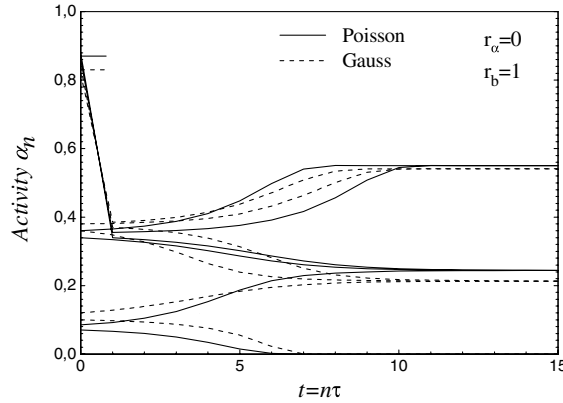
Figure 2. Time dependence of the total activity a_n for the netlet of Figure 1 with two chemical markers, a and b. Initial activities: $a_0 = 0.07, 0.085, 0.34, 0.36, 0.86, 0.88$ for the Poisson net and $a_0 = 0.1, 0.12, 0.36, 0.38, 0.82, 0.84$ for the Gaussian net.

In Figure 2 we monitor the time course of the total neural activity for the same netlet of Figure 1 for several time units (here $t = 15$). Several initial activities are chosen to exhibit as clearly as possible the stable and unstable steady-state levels. We notice here a critical point at high (initial) activities $a_0 = 0.87$ for the Poisson net ($a_0 = 0.83$ for the Gaussian net), for which a high initial neural activity above this level drops abruptly at the next time step to a region below the upper unstable steady-state level of neural activity, bringing the subsequent neural activity to the lower stable steady-state level, $a_{ss} = 0.24$ for the Poisson net. We observe that for the case of $a_0 = 0.87$ the activity sharply drops to a much lower level in the first step ($t = 1$). This is due to the fact that the nonzero refractory period yields a negative slope for the T-curve (total activity) at a_n values $a_n > 0.6$ (see Figure 1). We also notice that the nonzero Gaussian stable states are always lower than the corresponding Poisson states, while the Gaussian unstable steady-states are higher than those of the Poisson case. The Gaussian critical point, however, is lower than the corresponding one of the Poisson net.

The corresponding time delay diagrams for the above netlet with the same set of parameters are shown in Figure 3. These diagrams give the time, t_{ss}, that it takes for a netlet to reach a stable steady-state as a function of the initial activity. Here, unstable states are represented in general as 'peaks', while stable steady-states as 'wells'. The peak, however, at $a_0 = 0.87$ for the Poisson net (or at $a_0 = 0.83$ for the Gaussian net) corresponds to the above mentioned critical point of neural activity, which controls the time-course behavior of the netlet for high-level initial activities. If the activity at $t = 0$ is larger than 0.87 (see Figure 2), then the net will end up in the lower stable steady-state, $a_{ss} = 0.24$, instead of the highest, $a_{ss} = 0.55$. This effect is due to the refractoriness ($r_b = 1$) imposed on the larger marker, $m_b = 0.75$. Theoretically speaking, just as for unstable steady-states, one can prepare a network unable to reach a stable state. To do this one can give as an initial activity
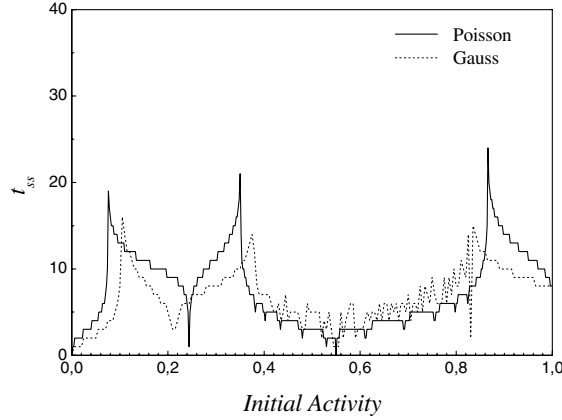
Figure 3. t_{ss}, the time it takes for the netlet to reach a stable steady-state versus the initial activity. Data shown are for the netlet of Figure 1 with two markers a and b. The solid lines are used for the Poisson approximation whereas the dashed lines for the Gaussian one.
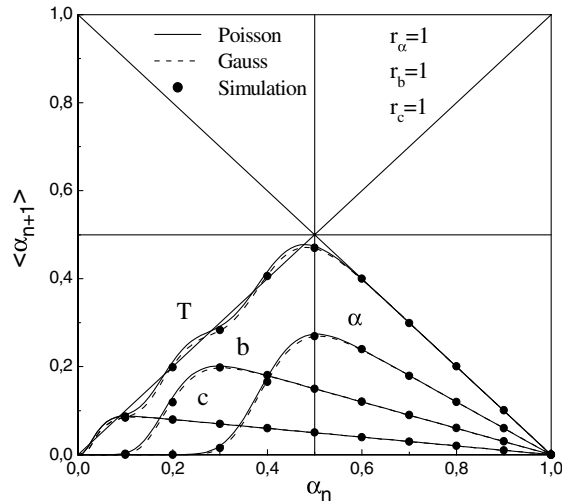

Figure 4. $\langle a_{n+1} \rangle$ versus a_n for an isolated netlet with three chemical markers, $m_\alpha = 0.6$, $m_b = 0.3$ and $m_c = 0.1$, with $\mu_\alpha^+ = 148$, $\mu_b^+ = 235$, $\mu_c^+ = 700$; $h = 0$; $\vartheta_\alpha = 36$, $\vartheta_b = 14$, $\vartheta_c = 3$; $r_a = 1$, $r_b = 1$, $r_c = 1$ and $K^+ = 1$. The curves a, b and c represent the activities of each marker, whereas T gives the total activity of the netlet. The solid lines are used for the Poisson approximation whereas the dashed lines for the Gaussian one. The solid dots are simulation results.

of the network the exact value of a critical point. In such a case at the next time step the activity will drop to the appropriate unstable steady-state remaining there indefinitely, unable to move to any stable state.

A second group of curves are plotted in Figures 4–6 for netlets with three markers $m_a = 0.6$, $m_b = 0.3$, $m_c = 0.1$. In Figures 4 and 5 we present plots of $\langle a_{n+1} \rangle$ versus a_n and time course diagrams for these nets with nonzero refractory periods for all of their subsystems ($r_a = 1$, $r_b = 1$, $r_c = 1$). In Figure 5, we show the Poisson
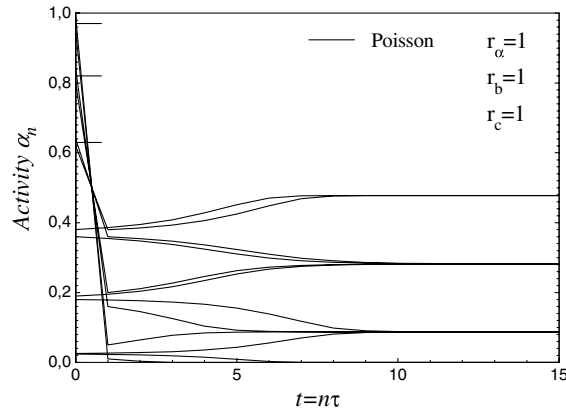
Figure 5. Time dependence of the total activity a_n for the netlet of Figure 4 with three chemical markers, a, b and c. Initial activities: $a_o = 0.024, 0.026, 0.18, 0.19, 0.36, 0.38, 0.62, 0.64, 0.8, 0.84, 0.95, 0.99$, for the Poisson approximation.
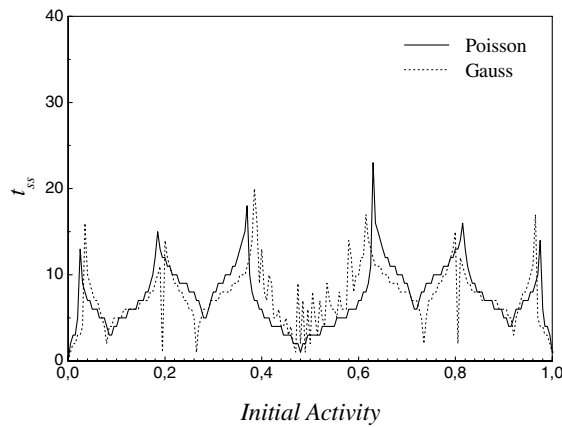

Figure 6. t_{ss}, the time it takes for the netlet to reach a stable steady-state versus the initial activity. Data shown are for the netlet of Figure 4 with three markers a, b and c. The solid lines are used for the Poisson approximation whereas the dashed lines for the Gaussian one.

approximation only, for more clearness. A similar representation we obtained for the Gaussian case not shown here. The time delay diagrams for the netlet of Figure 4 are shown in Figure 6.

In Figure 5, we can see three critical points at $a_o = 0.63, 0.82, 0.97$ for the Poisson net that control the subsequent resulting neural activity. In Figure 6 these points correspond to the three last peaks (to the right part of the figure) for the Poisson case. The behavior of the nets (Poisson and Gaussian) in these figures is similar to that of the previous nets with two markers, but now the three critical points lead the neural activity to stable steady-state levels, in inverse relation to their size, i.e. the higher the critical point, the lower is the final neural activity. This effect is due to the refractoriness ($r = 1$) imposed to all subsystems.

4.   Conclusions

In this paper we examined the effect of refractoriness on the dynamical steady-state behavior of pure Poisson or Gaussian first-order probabilistic neural nets. We have used neural nets in the spirit of mathematical models of our previous works as they were described in Section 2. They include explicitly separate domains of sub-populations characterized by chemical markers, as intercellular communication is restricted to occur among neurons that exhibit similar chemical affinity. Nevertheless, the calculations in this work, as shown by the analytical formulae (1–6), provide the possibility to observe both approximations, Poisson and Gaussian, of our models. Thus, we notice similar dynamical behavior in the two approximations and an excellent agreement between these data and the simulation results.

The significant point of interest, however, is the existence of some critical points at high neural activities (above the highest stable steady-state level), which control the subsequent resulting steady-state behavior of the net. An initial neural activity above a critical point leads to the appropriate lower stable steady-state level of neural activity. This is a phenomenon of neural net behavior which is analogous to the synchronized alpha-activity just before visual attention, which is usually well synchronized waves and which after attention becomes less synchronized with lower amplitudes [16]. We provided an explanation for the sharp drop in the activity, a_n, at early times. The emergence of the critical points and the resulting neural behavior are due to the nonzero refractory period imposed to the subsystems. In these models, the slope of neural activity, as we can see in Figures 1 and 4, is negative at high activities ($a_n > 0.6$), resulting to a reduction of subsequent neural activity. Using this mechanism we may interpret the observed abrupt drop of the neural activity, in the case of highly excited neural nets.

From a functional point of view the role of critical points is similar to that of the unstable steady-states, but they themselves do not represent steady-states. They, however, lead at once in the subsequent time step in unstable steady-states. Their feature, in contrast to the unstable steady-states, is that an initial activity above the level of any critical point leads the neural function to a lower stable steady-state, i.e. leads to a drop of activity to the appropriate lower level instead of the highest level of activity. For the case that the critical points are more than one, (as in the netlet with three markers of Figure 5, where three critical points appear), we notice an inverse relation of the initial activities to the resulting stable steady-state levels, according to the rule: 'The higher the critical point (initial activity), the lower is the resulting neural activity and the corresponding stable steady-state'. Thus, due to the refractoriness, external stimulation may provide a regulative result for the consequent neural activity, making the net to function in normal modes.

From the previously shown diagrams and other obtained results not exhibited here, we also conclude that the number of critical points for a netlet with N markers depends on the number of markers for which the refractory period is equal to one ($r = 1$). Thus, in a netlet with N markers each one of which has refractory

period, $r = 1$, there may appear up to N critical points, whereas in a netlet without any refractoriness there are no critical points. Furthermore, N-modal functions for the expectation value of activity (N-modal curves), and multiple hysteresis loops, or, equivalently, multiple states, can be obtained in a netlet with N markers without refractoriness ($r = 0$), as well as, in a netlet with N markers of nonzero refractory periods ($r = 1$) for all of its subsystems, i.e. the number of stable steady-states is independent of the existence of refractoriness. In this later case, however, the stable steady-states are all at levels below the value $a_{ss} = 0.5$. This restriction of the steady-state levels is another consequence of the existence of refractoriness, since the refractory period ($r = 1$) results to a relevant reduction of the stable steady-states of the net, due to the property imposed to the refractory active neurons, that causes them to be unable to fire in the next time step.

Acknowledgement

References

1. McCulloch, W. S. and Pitts, W.: A logical calculus of the ideas immanent in nervous activity, *Bulletin of Mathematical Biophysics*, **5** (1943), 115–133.
2. Caianiello, E. R.: Outline of a theory of thought-processes and thinking machines, *Journal of Theoretical Biology*, **2** (1961), 204–235.
3. Wilson, H. R. and Cowan, J. D.: Excitatory and inhibitory interactions in localized populations of model neurons, *Biophysics Journal*, **12** (1972), 1–24.
4. Griffin, J. S.: On the stability of brain-like structures, *Biophysics Journal*, **3** (1963), 299–309.
5. Harth, E. M., Csermely, T. J., Beek, B. and Lindsay, R. D.: Brain functions and neural dynamics, *Journal of Theortical Biology*, **26** (1970), 93–120.
6. Anninos, P. A., Beek, B., Csermely, T. J., Harth, E. M. and Pertile, G.: Dynamics of neural structures, *Journal of Theortical Biology*, **26** (1970), 121–148.
7. Anninos, P. A. and Kokkinidis, M.: A neural net model for multiple memory domains, *Journal of Theortical Biology*, **109** (1984), 95–110.
8. Adamopoulos, A. and Anninos, P. A.: Dynamic behavior of neural networks with chemical markers, *Connection Science*, **1** (1989), 393–402.
9. Fournou, E., Argyrakis, P. and Anninos, P. A.: Neural nets with markers and Gaussian-distributed connectivities, *Connection Science*, **5** (1993), 77–94.
10. Senn, W., Wyler, K., Streit, J., Larkum, M., Lüscher, H.-R., Mey, H., Müller, L., Stainhauser, D., Vogt, K. and Wannier, Th.: Dynamics of a random neural network with synaptic depression, *Neural Networks*, **9** (1996), 575–588.
11. Fournou, E., Argyrakis, P., Kargas, B. and Anninos, P. A.: Hybrid neural nets with Poisson and Gaussian connectivities, *Journal of Statistical Physics*, **89** (1997), 847–867.
12. Kotini, A. and Anninos, P. A.: Dynamics of noisy neural nets with chemical markers and Gaussian-distributed connentivities, *Connection Science*, **9** (1997), 381–403.
13. Prestige, M. C. and Willshaw, D. J.: On a role for competition in the formation of patterned neural connections, *Proceedings of the Royal Society of London B*, **90** (1975), 77–98.

14. Sperry, R. W.: Visumotor co-ordination in the newt (Triturus viridecens) after regeneration of the optic nerve, *Journal of Computational Neurology*, **79** (1943), 33–55.

15. Sperry, R. W.: Chemoaffinity in the orderly growth of the nerve fiber patterns and connections, *Proceedings of the National Academy of Sciences, USA,* **50** (1963), 703–709.

16. Ruch, T. C., Patton, H. D., Woodbury, J. W. and Towe, A. L.: Neurophysiology, W. B. Saunders Company, Philadelphia and London, 1968.